Available online at www.sciencedirect.com
SCIENCE DIRECT®
Optics Communications 257 (2006) 76–83
OPTICS COMMUNICATIONS
www.elsevier.com/locate/optcom

Pressure and power broadening of the a_{10} component of R(56) 32-0 transition of molecular iodine at 532 nm

Hui-Mei Fang [a,*], S.C. Wang [a,1], Jow-Tsong Shy [b]

[a] Department of Photonics and Institute of Electro-Optical Engineering, National Chiao Tung University, Hsinchu 300, Taiwan, ROC
[b] Department of Physics and Institute of Photonics Technologies, National Tsing Hua University, Hsinchu 300, Taiwan, ROC

Received 21 February 2005; received in revised form 28 April 2005; accepted 5 July 2005

Abstract

We determine the linewidth of the hyperfine structure a_{10} component of R(56) 32-0 transition of $^{127}I_2$ at 532 nm using the dependence of the peak amplitude of the third-derivative signal on the modulation width. We also use the same method to investigate pressure broadening and power broadening of the a_{10} component.

PACS: 33.20

Keywords: Nd:YAG laser; Saturation spectroscopy; Pressure broadening; Power broadening; Phase sensitive detection

1. Introduction

Optical frequency standards are of great interest not only for metrology applications but also for high-resolution spectroscopy, optical communications and fundamental physics. In recent years diode-pumped solid state laser systems have been targeted as the ideal sources for optical frequency standards. The diode-pumped, frequency doubled Nd:YAG laser at 532 nm has generated a great deal of interests due to its inherently low frequency noise, small size, high reliability, and relatively high powers. Since the observation of hyperfine components of iodine transitions near 532 nm and the laser frequency stabilization based on the observed transitions using FM side-band spectroscopy [1,2], iodine-stabilized Nd:YAG lasers have demonstrated stabilities better than the 633 nm iodine-stabilized He–Ne lasers [3].

* Corresponding author. Tel.: +886 3 5742561; fax: +886 3 5723052.
E-mail addresses: fhm590425@yahoo.com (H.-M. Fang), scwang@cc.nctu.edu.tw (S.C. Wang), shy@phys.nthu.edu.tw (J.-T. Shy).
[1] Tel.: +886 3 5712121x56320; fax: +886 3 5716631.

0030-4018/$ - see front matter © 2005 Elsevier B.V. All rights reserved.
doi:10.1016/j.optcom.2005.07.016

The 2001 meeting of consultative committee for length (CCL) led the a_{10} component of R(56) 32-0 transition of $^{127}I_2$ at 532 nm for the optical frequency standard [4]. It will be the most important wavelength standard in the visible range in the future. Its pressure shift and power shift has been reported [5]. However, the characteristics of the a_{10} component including linewidth, pressure broadening, and power broadening have not been investigated systematically.

In this paper, we use the dependence of the peak amplitude of the third-derivative signal on the modulation width (PAM from now on) to determine the linewidth of the a_{10} component, and also investigate its pressure and power broadened. To verify the accuracy of this linewidth determination method, we measure the full-width at half-maximum (FWHM) linewidth of the a_{10} component using the conventional saturation spectroscopy method. The experimental line profile obtained using the saturation spectroscopy method is fitted with Lorentzian profile. The fitted linewidth is in good agreement with the linewidth determined by PAM. The linewidth of the a_{10} component under different pressure and power have also been determined using PAM. The slope of the linear fit for pressure broadening is 63 kHz/Pa. The power broadening parameter shows the saturation intensity is 5.76 mW/mm^2.

2. Theoretical background

Line profiles are often investigated by means of a modulation process. By this process the static profile is converted into a periodically alternating signal allowing the well-established techniques of phase sensitive detection (PSD) to be applied. PSD produces a derivative of the line profile, that is, one of the harmonics that appear at the RF output, by sweeping the field frequency with a certain amount of frequency modulation. Consequently, the demodulated signal depends on the form of the line profile and also on the amplitude and the spectral purity of the modulation. The demodulated signals have been derived on the assumption of a pure harmonic modulation [6,7]. We will briefly review the derivation following the work by Bayer-Helms and Helmcke [6].

The line profile may be mathematically described by a function $f(d)$, in which d is the modulated quantity measured in intervals of the frequency. At first an exactly harmonic modulation

$$d = d_M + d_A \cos \omega t \tag{1}$$

may be assumed at the instantaneous mean value $d = d_M$ with the modulation amplitude $d_A(>0)$ and the modulation angular frequency ω. The periodic signal can be expressed by a Fourier series

$$f(d_M + d_A \cos \omega t) = A_0/2 + \sum_{m=1}^{\infty} (A_m \cos m\omega t + B_m \sin m\omega t). \tag{2}$$

The corresponding Fourier coefficients or signal coefficients A_m and B_m give the amplitudes of the higher harmonics in the signal as well as their phase relations to the modulation (1). They are calculable according to equation

$$A_m + iB_m = 1/\pi \int_0^{2\pi} f(d_M + d_A \cos \omega\tau)\, e^{im\omega\tau}\, d\tau, \quad m \geqq 0 \tag{3}$$

if the profile function $f(d)$ is known. By bisection of the interval 2π of the integrals in (3) one obtains

$$A_m = 2/\pi \int_0^{\pi} f(d_M + d_A \cos \omega\tau) \cos(m\omega\tau)\, d\tau, \quad B_m = 0, \tag{4}$$

which means that if the modulation is described by $\cos \omega t$, the phase relations of all harmonics are always given by $\cos m\omega t$.

For Lorentzian profile

$$f(d) = 1/(1 + \delta^2). \tag{5}$$

The symbol δ designates the dimensionless quantity of d divided by the half-width at half-maximum d_H

$$\delta = d/d_H, \quad \delta_M = d_M/d_H, \quad \delta_A = d_A/d_H. \tag{6}$$

The Fourier coefficient A_m gives the amplitude of the higher-derivative signal of the Lorenzian line profile. The first four Fourier coefficients for the Lorentzian profile are [6]

$$P_{\pm} = (2(\rho \pm \alpha))^{0.5}/\rho, \qquad \rho = (\alpha^2 + 4\delta_M^2)^{0.5},$$
$$\alpha = 1 + \delta_A^2 - \delta_M^2, \tag{7}$$
$$A_0 = P_+, \tag{8}$$
$$A_1 = ((\operatorname{sgn}\delta_M)P_- - \delta_M P_+)/\delta_A, \tag{9}$$
$$A_2 = (-4|\delta_M|P_- - (2(1-\delta_M^2)+\delta_A^2)P_+ + 4)/\delta_A^2, \tag{10}$$
$$A_3 = ((-\operatorname{sgn}\delta_M)(4(1-3\delta_M^2)+3\delta_A^2)P_- + (4(3-\delta_M^2) + 3\delta_A^2)\delta_M P_+ - 16\delta_M)/\delta_A^3. \tag{11}$$

The analytical form of the peak amplitude of the first-derivative signal on the normalized modulation width δ_A has been derived by Nakazawa [7]. The formula is as follows:

$$f(\delta_A) = \frac{\sqrt{3}[(4+3\delta_A^2)^{1/2} - 2]}{2\delta_A[(4+3\delta_A^2)^{1/2} - 1]^{1/2}}. \tag{12}$$

For the second- and third-derivative signals, no analytical formula has been derived for the peak amplitude on the modulation width. We can obtain the second-derivative signal as a function of δ_M for different δ_A using Eq. (10), we then determine the peak amplitude from the second-derivative signal. We propose following analytical formula for the peak amplitude vs. the normalized modulation width:

$$g(\delta_A) = (P_1\delta_A + P_2\delta_A^2)/(P_3 + P_4\delta_A + P_5\delta_A^2 + P_6\delta_A^3). \tag{13}$$

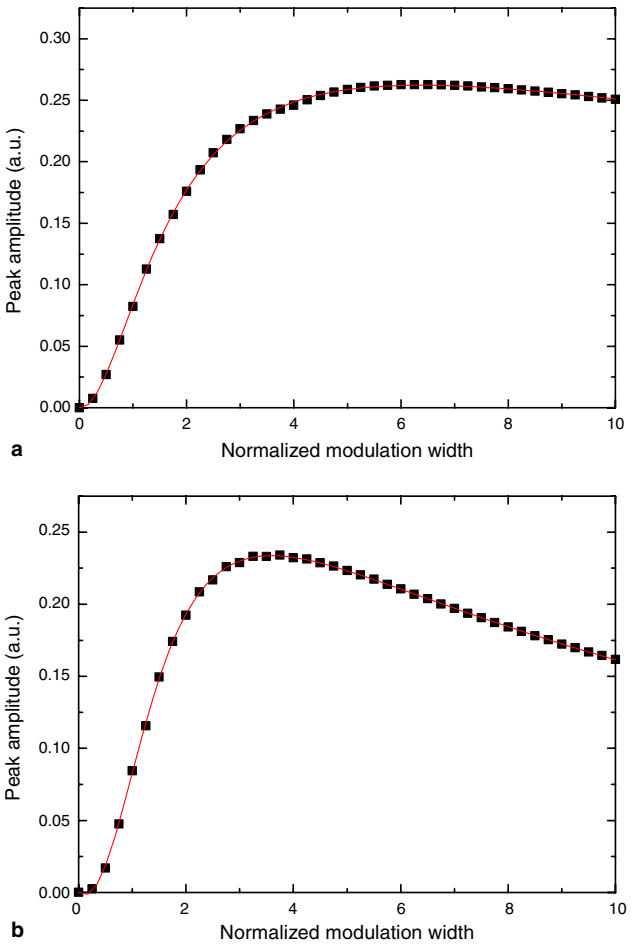

Fig. 1. (a) The peak amplitude of the second-derivative signal vs. the normalized modulation width (dotted points) and the curve of the analytical function $g(\delta_A)$ (solid line). (b) The peak amplitude of the third-derivative signal vs. the normalized modulation width (dotted points) and the curve of the analytical function $h(\delta_A)$ (solid line).

The fitted coefficients are $P_1 = -0.06795$, $P_2 = 1.20627$, $P_3 = 7.688$, $P_4 = 2.63378$, $P_5 = 3.11903$, $P_6 = 0.13152$. Fig. 1(a) shows the peak amplitude of the second-derivative signal as a function of the normalized modulation width (dotted points) and the curve of the analytical function $g(\delta_A)$ (solid line).

The peak amplitude of the third-derivative signal on the normalized modulation width is also analyzed similarly. The analytical function is

$$h(\delta_A) = (P_1\delta_A + P_2\delta_A^2 + P_3\delta_A^3) / (P_4 + P_5\delta_A + P_6\delta_A^2 + P_7\delta_A^3). \quad (14)$$

The fitted coefficients are $P_1 = -1.51636$, $P_2 = 6.89591$, $P_3 = -0.09229$, $P_4 = 48.96763$, $P_5 = -3.70996$, $P_6 = 16.56378$, and $P_7 = 1.93711$. Fig. 1(b) shows the peak amplitude of the third-derivative signal as a function of the normalized modulation width (dotted points) and the curve of the analytical function $h(\delta_A)$ (solid line). The difference between the peak amplitude and the analytical function curve is less than 1% for both analytical functions $g(\delta_A)$ and $h(\delta_A)$.

3. Experimental setup

The experimental setup is shown in Fig. 2. We use a 450-mW monolithic diode-pumped non-planar ring oscillator (NPRO) Nd:YAG laser (Lightwave Electronics Model 126) as the light source. The NPRO laser has the good characteristics of narrow linewidth (less than 5 kHz), low frequency drifts (less than 50 MHz/h), and wide single mode tuning range (larger than 35 GHz). Its frequency can be tuned by changing the temperature of the laser crystal (thermal tuning), or applying a voltage on the piezoelectric transducer (PZT) attached on the laser crystal. The former has a slow response time of few seconds and the latter has a response bandwidth of 100 kHz.

The laser beam passes through a 30-dB Faraday isolator to reduce the optical feedback effect and then passes through a half-wave plate ($\lambda/2$) into a periodically poled $LiNbO_3$ (PPLN) crystal. The PPLN crystal is 50-mm long and 0.5-mm thick with a 6.5-μm period. The PPLN is heated to 53 °C for quasi-phase-matched frequency doubling. The $\lambda/2$ is used to adjust the light polariza-

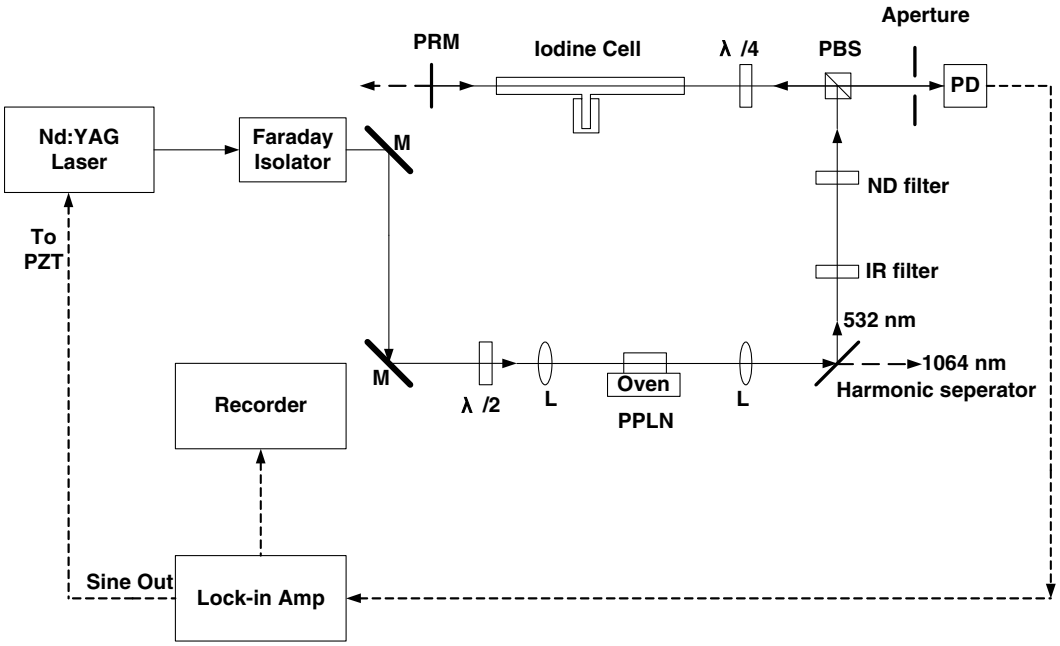

Fig. 2. Experimental setup: M, mirror; $\lambda/2$, half-wave plate; L, lens; PPLN, periodically poled $LiNbO_3$; ND filter, neutral density filter; PBS, polarizing beam splitter; $\lambda/4$, quarter-wave plate; PRM, partial reflection mirror; PD, photodiode.

tion to match the PPLN z-direction. The output wavelengths from the PPLN crystal include fundamental 1064 nm and second harmonic 532 nm. They are separated by a harmonic separator. This harmonic separator is a dichroic beam splitter which separates the Nd:YAG fundamental from its second harmonic. The 1064 nm beam is transmitting and the other 532 nm beam is reflected. Then the 532 nm beam passes through an IR filter to further filter out the residual 1064 nm radiation. The 532 nm laser output then enters a 10-cm long iodine cell as the pump beam. A neutral density (ND) filter is used to adjust the power of the pump beam. A fraction of the pump beam reflected from a 40% partial reflection mirror (PRM) is the probe beam. The probe beam is detected by a photodiode after passing through a quarter-wave plate ($\lambda/4$) and a polarizing beam splitter (PBS).

The Doppler-free saturation spectrum of hyperfine components of R(56) 32-0 transition is observed using the conventional third-harmonic demodulation method with a lock-in amplifier and is recorded by a chart recorder. The lock-in amplifier we use is SR830 from Stanford Research Systems which has the ability to demodulate the signal at any harmonic up to 19,999. In our experiment, we use the sine out of the lock-in amplifier at 10 kHz to modulate the Nd:YAG laser frequency and choose the third-harmonic of 10 kHz (i.e., 30 kHz) to demodulate a_{10} signal. The time constant of the lock-in amplifier is 300 μs. The laser frequency is scanned by applying a triangular signal to the PZT.

4. Results and discussion

We first use the a_{10} component of R(56) 32-0 transition to check the PAM method. The third-derivative signal of a_{10} is obtained using the third-harmonic demodulation method. The pump beam power is 4.75 mW and the vapor pressure of the iodine cell keeps at about 4.1 Pa. The pump beam size in the center of the iodine cell is about 1.3 mm in diameter. When the Nd:YAG laser is modulated by the sine output from the lock-in amplifier, we record the third-derivative signal of hyperfine component a_{10}. We then measure the peak amplitude of the third-derivative signal.

Fig. 3 shows the peak amplitude of the third-derivative signal vs. the modulation width. The dotted points are the experimental data. We determine the linewidth by fitting the experimental points to equation $h(\delta_A)$ (Eq. (14)). The solid line in Fig. 3 is the fitted curve. The experimental data agree with the fitted curve are very well. The FWHM width of the a_{10} component determined

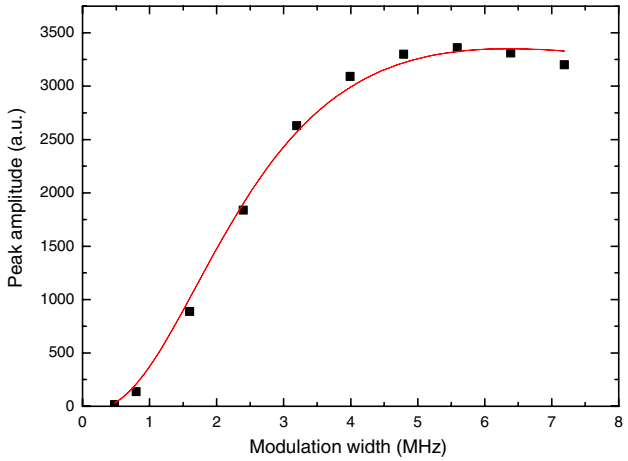

Fig. 3. The measured peak amplitude of the third-derivative signal vs. modulation width (dotted points) and the fitted curve (solid line). The fitted FWHM width of the a_{10} component is 1.755 ± 0.044 MHz.

by PAM is 1.755 MHz with a standard deviation of 0.044 MHz.

To verify the PAM measurement, we measure the a_{10} linewidth using the saturation spectroscopy method. The experimental setup is shown in Fig. 4(a). The second-harmonic 532 nm beam after PPLN is divided into two beams with 1.5 and 6.5 mW respectively. We lock the Nd:YAG laser to the a_6 component of R(56) 32-0 transition using the 1.5-mW beam. The experimental setup shown

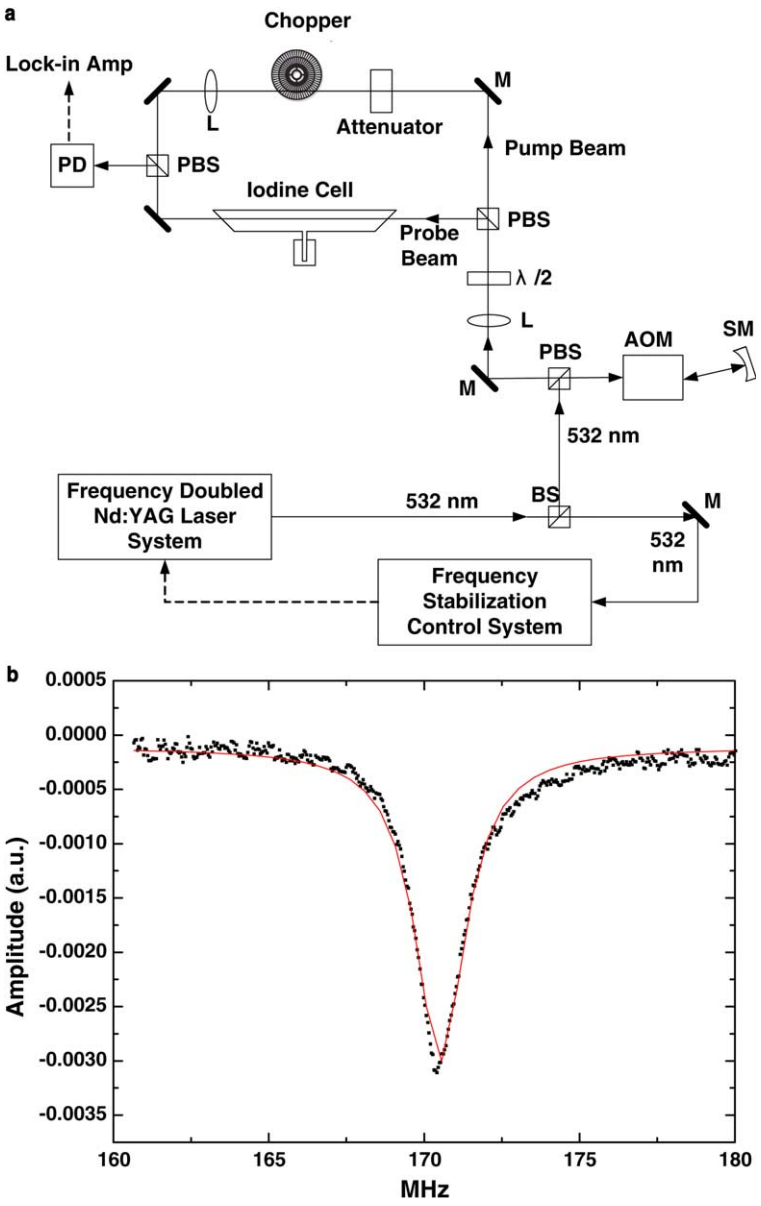

Fig. 4. (a) Experimental setup for saturation spectroscopy of the a_{10} component of R(56) 32-0 transition: BS, beam splitter; M, mirror; $\lambda/2$, half-wave plate; L, lens; PBS, polarizing beam splitter; PD, photodiode; AOM, acousto-optic modulator; SM, spherical mirror (concave). (b) Saturation spectrum of the a_{10} component. The solid line is the fitted Lorentzian profile. The fitted FWHM width is 1.952 ± 0.018 MHz.

in Fig. 2 is used to obtain the third-derivative signal for stabilizing the laser frequency. The 6.5-mW beam enters a double-passed acousto-optic modulator (AOM) frequency shifter to generate a frequency tunable beam. This frequency shifted beam is used to scan the saturation spectroscopy of the a_{10} component of R(56) 32-0 transition. Fig. 4(b) shows the saturation spectrum of the a_{10} component. For comparison, we carefully adjust the intensities of the pump and probe beams such that they equal to the intensities used in PAM. We also apply a sine modulation with proper phase to the AOM frequency shifter to reduce the laser frequency modulation. The observed saturation spectrum is fitted with Lorentzian profile and the fitted FWHM linewidth is 1.952 ± 0.018 MHz. The observed lineshape shows a little asymmetric. It is probably due to the non-constant background. It requires further study in the future. Because the 532 nm laser beam after the double-passed AOM frequency shifter has a linewidth of 0.18 MHz (measured by beating with another unmodulated frequency-doubled Nd:YAG laser). Therefore, the FWHM linewidth of the a_{10} component is 1.772 MHz (i.e., 1.952-D 0.18 MHz) [8,9]. This value is in agreement with the linewidth of 1.755 MHz using PAM within the uncertainty.

After verifying the PAM method for linewidth determination, we use it to investigate the variation of the linewidth of a_{10} with respect to the laser power and the vapor pressure of iodine. To investigate the variation of the linewidth with respect to vapor pressure of the iodine cell, we fix the pump power at 4.75 mW and vary the cold finger temperature of the iodine cell from -8.32 °C (vapor pressure = 1.74 Pa) to 10 °C (vapor pressure = 10.86 Pa). The variation of the a_{10} linewidth with iodine vapor pressure is shown in Fig. 5. The FWHM linewidth varies from 1.657 to 2.219 MHz. The slope of the linear fit is 63 ± 2 kHz/Pa for FWHM linewidth. For comparison, pressure broadening is 106 kHz/Pa for the b_{15} component of P(48) 11-3 transition [10] and is 148 kHz/Pa for the a_1 component of R(56) 32-0 transition [11].

To investigate the variation of the linewidth due to laser power, we adjust pump power from 0.19 to 4.75 mW and fix cold finger temperature of the iodine cell at -0.58 °C (vapor pressure = 3.9 Pa). The probe power is 27% of the pump power. The variation of the a_{10} linewidth with pump power is shown in Fig. 6. The FWHM linewidth increases from 1.482 to 1.690 MHz. The linewidth and pump power have following relation [11,12]:

$$\gamma' = \gamma(1 + \sqrt{(1 + P/P_S)}), \tag{15}$$

where γ is the FWHM linewidth associated with the limit of weak saturating and probe beams, P is the pump power, and P_S is the saturating power.

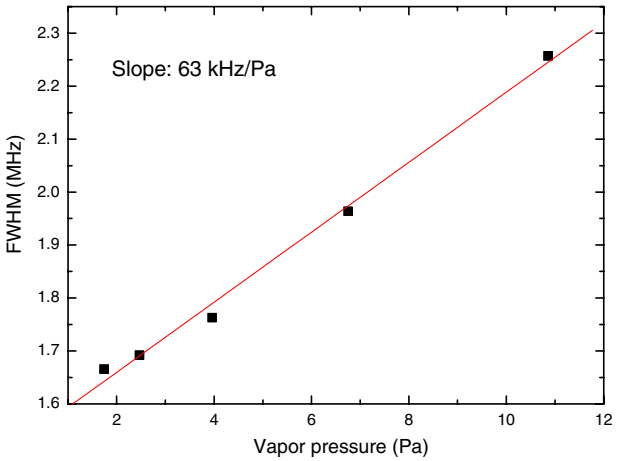

Fig. 5. The a_{10} linewidth vs. vapor pressure of the iodine cell. The pump power is fixed at 4.75 mW. The pressure broadened linewidth is quite linear with a slope of 63 ± 2 kHz/Pa.

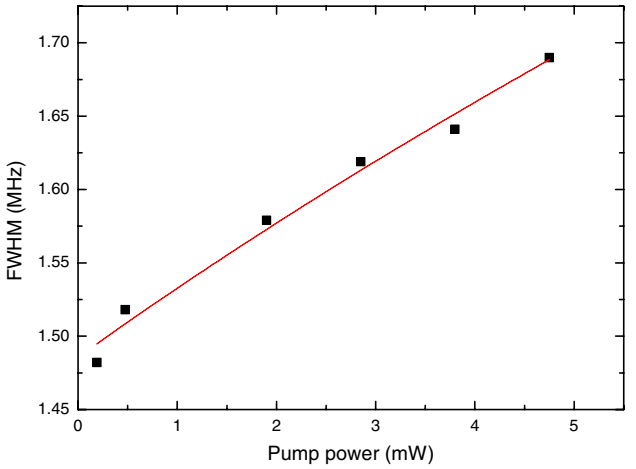

Fig. 6. The a_{10} linewidth vs. pump power. The cold finger temperature of the iodine cell is fixed at −0.58 °C (vapor pressure = 3.9 Pa). The fitted results are $\gamma = 0.74 \pm 0.007$ MHz and $P_S = 7.65 \pm 0.56$ mW.

Using a nonlinear least-squares fit to the data shown in Fig. 6, we obtain that γ is 0.74 MHz and P_S is 7.65 mW. Since the diameter of the pump beam in the center of the iodine cell is about 1.3 mm, the saturation intensity is about 5.76 mW/mm^2. For comparison, the FWHM linewidth of the a_1 component of R(56) 32-0 transition is 0.288 MHz at the vapor pressure of 1.4 Pa and its pressure broadening is 148 kHz/Pa [11]. Consequently, the a_1 linewidth at the vapor pressure of 3.9 Pa is about 0.66 MHz. Our fitted a_{10} linewidth of 0.74 MHz at 3.9 Pa is close to it.

5. Conclusions

We have verified that the Lorentzian linewidth can be easily determined by using the dependence of the peak amplitude of the third-derivative signal on the modulation width (PAM). We have also used this method to investigate pressure broadening and power broadening of the a_{10} component of R(56) 32-0 transition of $^{127}I_2$ at 532 nm systematically. The pressure broadened linewidth is quite linear with vapor pressure. The slope of the linear fit is 63 kHz/Pa for FWHM width. From the power broadening parameter the saturation intensity is obtained to be 5.76 mW/mm^2.

References

[1] A. Arie, S. Schiller, E.K. Gustafson, R.L. Byer, Opt. Lett. 17 (1992) 1204.
[2] A. Arie, R.L. Byer, J. Opt. Soc. Am. B 10 (1993) 1990.
[3] J.L Hall, L.-S. Ma, M. Taubman, B. Tiemann, F.-L. Hong, O. Pfister, J. Ye, IEEE Trans. Instrum. Meas. 48 (1999) 583.
[4] T.J. Quinn, Metrologia 40 (2003) 103.
[5] K. Nyholm, M. Merimaa, T. Ahola, A. Lassila, IEEE Trans. Instrum. Meas. 52 (2003) 284.
[6] F. Bayer-Helms, J. Helmcke, PTB-Bericht. Me 17 (1977) 85.
[7] M. Nakazawa, J. Appl. Phys. 59 (1986) 2297.
[8] J.H. Eberly, Phys. Rev. Lett. 37 (1976) 1387.
[9] A.T. Georges, P. Lambropoulos, Phys. Rev. A 18 (1978) 587.
[10] M. Gläser, Metrologia 23 (1986) 45.
[11] M.L. Eickhoff, J.L. Hall, IEEE Trans. Instrum. Meas. 44 (1995) 155.
[12] V.S. Letokhov, V.P. Chebotayev, Nonlinear Laser Spectroscopy, Springer, Berlin, 1977, p. 72.